PAPER

Comparison of cardiac magnetic resonance imaging and bio-impedance spectroscopy for the assessment of fluid displacement induced by external leg compression

IOP Publishing | Institute of Physics and Engineering in Medicine Physiological Measurement

Physiol. Meas. **38** (2017) 15–32 doi:10.1088/1361-6579/38/1/15

Comparison of cardiac magnetic resonance imaging and bio-impedance spectroscopy for the assessment of fluid displacement induced by external leg compression

Salvatore Saporito[1,5], Silviu Dovancescu[1,2,5], Ingeborg H F Herold[1,3], Harrie C M van den Bosch[4], Hans C van Assen[1], Ronald M Aarts[1,2], Hendrikus H M Korsten[1,3] and Massimo Mischi[1]

[1] Department of Electrical Engineering, Eindhoven University of Technology, Den Dolech 2, 5612 AZ, Eindhoven, The Netherlands
[2] Philips Research, Eindhoven, The Netherlands
[3] Department of Anesthesiology and Intensive Care, Catharina Hospital Eindhoven, Eindhoven, The Netherlands
[4] Department of Radiology, Catharina Hospital Eindhoven, Eindhoven, The Netherlands

E-mail: s.saporito@tue.nl

Received 3 May 2016, revised 20 September 2016
Accepted for publication 20 October 2016
Published 12 December 2016

Abstract

Heart failure is marked by frequent hospital admissions, often as a consequence of pulmonary congestion. Current gold standard techniques for thoracic fluid measurement require invasive heamodynamic access and therefore they are not suitable for continuous monitoring. Changes in thoracic impedance (TI) may enable non-invasive early detection of congestion and prevention of unplanned hospitalizations. However, the usefulness of TI to assess thoracic fluid status is limited by inter-subject variability and by the lack of reliable normalization methods. Indicator dilution methods allow absolute fluid volume estimation; cardiac magnetic resonance (CMR) has been recently proposed to apply indicator dilution methods in a minimally-invasive manner.

In this study, we aim to compare bio-impedance spectroscopy (BIS) and CMR for the assessment of thoracic fluid status, and to determine their ability to detect fluid displacement induced by a leg compression procedure in healthy volunteers.

[5] The first two authors contributed equally to this article.

A pressure gradient was applied across each subject's legs for 5 min (100–60 mmHg, distal to proximal). Each subject underwent a continuous TI-BIS measurement during the procedure, and repeated CMR-based indicator dilution measurements on a 1.5 T scanner at baseline, during compression, and after pressure release. The Cole–Cole and the local density random walk models were used for parameter extraction from TI-BIS and indicator dilution measurements, respectively. Intra-thoracic blood volume index (ITBI) derived from CMR, and extracellular fluid resistance (R_E) from TI-BIS, were considered as thoracic fluid status measures.

Eight healthy volunteers were included in this study. An increase in ITBI of $45.2 \pm 47.2\,\text{ml m}^{-2}$ was observed after the leg inflation ($13.1 \pm 15.1\%$ w.r.t. baseline, $p < 0.05$), while a decrease of $-0.84 \pm 0.39\,\Omega$ in R_E ($-1.7 \pm 0.9\%$ w.r.t. baseline, $p < 0.05$) was observed. ITBV and R_E normalized by body mass index were strongly inversely correlated ($r = -0.93$, $p < 0.05$).

In conclusion, an acute fluid displacement to the thoracic circulation was induced in healthy volunteers. Significant changes were observed in the considered thoracic fluid measures derived from BIS and CMR. Good correlation was observed between the two measurement techniques. Further clinical studies will be necessary to prospectively evaluate the value of a combination of the two techniques for prediction of re-hospitalizations after admission for heart failure.

Keywords: bio-impedance spectroscopy, intra-thoracic blood volume, thoracic impedance, cardiac magnetic resonance, indicator dilution theory, thoracic fluid monitoring

(Some figures may appear in colour only in the online journal)

Introduction

Hospitalizations due to acute heart failure (HF) are a major health problem (Blair *et al* 2009, Karamitsos *et al* 2009); hospital admissions and re-admissions are mainly related to fluid congestion (Blair *et al* 2009, Picano *et al* 2010). Research has shown that congestion precedes symptoms by weeks (Adamson *et al* 2003, Yu *et al* 2005, Chaudhry *et al* 2007, Cotter *et al* 2008, Gheorghiade *et al* 2010). It has been suggested that the mechanism of fluid congestion in HF patients relates to fluid redistribution to the lungs rather than to fluid accumulation (Cotter *et al* 2008). Early detection of fluid congestion would therefore improve the management of HF patients (O'Connor *et al* 2005, Picano *et al* 2010).

Variations in body weight anticipate hospitalization for HF (Chaudhry *et al* 2007, Gheorghiade *et al* 2012). However, studies have shown that body weight changes during an acute HF episode (Cotter *et al* 2008) are minimal and they relate poorly to improvement in patients' symptoms during therapy (Gattis *et al* 2004, Blair *et al* 2009) since they may not always reflect changes in intravascular volumes (Blair *et al* 2009).

Pulmonary capillary wedge pressure (PCWP) has also been used to assess pulmonary fluid status (Gheorghiade *et al* 2010). However, the values of PCWP as an indirect volume measure has recently been questioned, as altered fluid status can be present also in the presence of normal PCWP values (Katz 2007).

The accumulation of intra-thoracic fluid causes a decrease in thoracic impedance (TI) (Yancy and Abraham 2003, Katz 2007) that can be detected by applying electrical currents across the thorax. Several studies have shown a consistent reduction in TI during congestion, potentially providing a measurement technique for early warning systems to anticipate acute HF decompensation (Yu *et al* 2005, Gheorghiade *et al* 2010, Weyer *et al* 2014). TI strongly correlated with fluid changes after intravenous diuretic administration (Conraads *et al* 2011).

However, TI is also influenced by adiposity, muscularity, height, intrinsic lung characteristics, and electrode placement (Bolton *et al* 1998, Katz 2007, Sasaki *et al* 2013). This may explain the relatively low sensitivity for prediction of HF events reported in several trials (Conraads *et al* 2011, van Veldhuisen *et al* 2011, Heist *et al* 2014, Gyllensten *et al* 2016a). It is likely that there is some individual variability in the optimal threshold in TI changes to detect fluid accumulation, requiring personalization of this setting for individual patients (Abraham *et al* 2011, Gyllensten *et al* 2016b).

Recently, prototypes of wearable systems for continuous, non-invasive monitoring of TI have been proposed (Medrano *et al* 2007, Zlochiver *et al* 2007) using surface electrodes. However, TI measured on the body surface is affected also by changes in skin preparation, differences in electrode placement (Yu *et al* 2005), and subject posture (Scharfetter *et al* 1997, Medrano *et al* 2007, Dovancescu *et al* 2013).

Bio-impedance spectroscopy (BIS) consists in the measurement of bio-impedance over multiple frequencies. BIS provides information about tissue characteristics (e.g. intra- and extracellular fluid volumes, fat mass, muscle mass) and has been widely used for the assessment of body composition (Kushner 1992, Moissl *et al* 2006). The measurement principle relies on the frequency-dependent behavior of body tissues: low frequency currents flow around the cells through the extracellular fluid; high frequency currents also flow through the capacitive cell membranes and the intracellular fluid (Scharfetter *et al* 1997, Bera 2014). BIS should be measured over a wide frequency range; however, for technical reasons, usually a limited frequency range is used and resistances of extracellular and intracellular fluids are then extrapolated to zero and infinite frequencies, respectively (Kanai *et al* 1987, Jaffrin and Morel 2008). Extrapolation is facilitated by the observation that the impedance data distribute as a semi-circle in the resistance–reactance plane, according to the Cole–Cole model (Cole and Cole 1941).

So far, no reliable normalization methods are available for the comparison of TI measurements between subjects. The clinical utility of TI measurements is therefore limited to the observation of relative changes over time within subjects (Katz 2007, Jaffrin *et al* 1997), thus providing only an additional tool for managing HF in patients with implanted devices.

Reference methods for measuring absolute body fluid volumes directly are based on dilution of radioisotopes (Schloerb *et al* 1950, Pierson *et al* 1982). Dilution-based measurements have been shown to be sensitive to volume changes during surgical interventions (Slutsky *et al* 1983), and to correlate well with measurements of filling pressures in decompensated HF patients (Gheorghiade *et al* 2010). In these methods, a suitable indicator is injected in the circulation. By sampling the concentration of the indicator, indicator dilution curves (IDCs) can be derived. The central volume theorem (Stewart 1921) relates fluid volumes and IDC parameters, which can be derived by model fitting (Harabis *et al* 2013). Depending on the intravascular or extravascular character of the used indicator, the derived volume measurements will only include blood volumes or take into account also extravascular fluids. In order to distinguish between pulmonary blood volumes and extravascular fluid volumes, often a combination of intravascular and extravascular indicator is used (Sakka *et al* 2000); alternatively, physiological modelling allows separation of the two compartments using only one extravascular contrast agent (Sakka *et al* 2000). Methods using ionizing tracers have limited

clinical applicability; even with the use of non-ionizing indicators such as dye or cold saline, the method remained invasive, as central vessel catheterization was required to sample the indicator concentration.

More recently, imaging contrast agents (CAs) have been proposed as indicators that enable the application of the method in a minimally invasive way (Mischi *et al* 2004, Lakoma *et al* 2010). In particular, cardiac magnetic resonance (CMR), the current gold standard imaging technique for the assessment of HF (Karamitsos *et al* 2009), allows measuring blood flow using phase contrast-MRI sequences (Wong 2014), and indicator dilution measurement using gadolinium-based CAs and dynamic contrast-enhanced MRI (DCE-MRI) sequences (Mischi *et al* 2009). CMR is therefore a promising minimally-invasive alternative for absolute thoracic fluid volume measurement. As gadolinium-based CAs freely distribute to the extracellular space (Aime and Caravan 2009), similarly to BIS, indicator dilution estimates based on DCE-MRI are influenced by interstitial fluids.

The costs associated with CMR limit its applicability for patient follow-up. However, the ability to intermittently determine absolute fluid volumes might complement measurement techniques able to continuously track relative changes (Katz 2007).

In this study, we aim at comparing BIS and CMR for the assessment of thoracic fluid status and to determine their sensitivity to fluid displacement obtained through a leg compression maneuver. We introduce an experimental design to induce rapid and reversible fluid displacement in healthy subjects by means of a pneumatic compression device, which excludes confounding factors associated with postural maneuvers. We present the effects of the compression procedure on TI and on CMR measurements and delineate a comparison between the two techniques based on data collected in healthy volunteers.

Materials and methods

Study population

The study was carried out at the Radiology Department of the Catharina Hospital Eindhoven, the Netherlands. The protocol was approved by the local medical ethics committee and registered as a clinical trial on clinicaltrials.gov (NCT02364193). All participants provided written informed consent at enrollment. Eligible for the study were healthy adults (age $\geqslant$18 years) without known history of cardiovascular pathologies, and with body mass index (BMI) between 18 and 25. Exclusion criteria were poor renal function quantified by a glomerular filtration rate $<$60 ml min^{-1}, and the presence of the general contraindications for use of gadolinium-based CAs.

Eligible subjects were requested to attend two repeated sessions of external leg compression applied in supine position. Subjects were monitored using BIS in one session and CMR in the other. Between sessions, the subjects engaged in common activities of daily life for approximately 2 h, in order to reduce any potential mutual influence between the two procedures. The order of the sessions was randomized.

Leg compression procedure

Passive leg raising, a common physiological maneuver used in intensive care, involves assisted raising of the legs from the horizontal position to a tilted one, to produce a gravitational displacement of blood from the lower limbs towards the thorax (Monnet *et al* 2006). The use of passive leg raising as a fluid displacement technique introduces undesirable effects which may

confound BIS measurements: abdominal organs, which have a lower resistance then the lungs, advance towards the thoracic cage while the thoracic contour is modified (Cassola *et al* 2010). Similar considerations apply to head down tilt maneuvers (Henderson *et al* 2009). Additionally, these maneuvers would be unpractical to perform within a closed-bore MRI scanner.

To exclude confounding factors we induced fluid displacement by means of external leg compression with a Lympha-mat Digital (Bösl Medizintechnik, Aachen, Germany) gradient pump system. The system includes an automatic air pump and a pair of inflatable leg sleeves. Each sleeve is composed of 12 overlapping air-chambers which are inflated individually in temporal succession, from distal to proximal (foot to upper leg). The gradual inflation of both leg sleeves starts simultaneously and ends when the pressure in each of the air chambers reaches a predefined value. In our study, the pressure applied to the sleeves was distributed with a spatial gradient along the leg, such that at the end of the inflation, the pressure in the four most distal chambers was 100 mmHg, in the four intermediate chambers 80 mmHg, and in the four proximal chambers 60 mmHg. Under normal operation conditions, the device automatically releases the pressure from all chambers simultaneously after the target pressure profile is reached and restarts with the inflation. For this study, the device was modified to hold the pressure in the leg sleeves after maximum inflation was achieved and to release the pressure only on manual command. At the beginning of each session, participants put on the deflated leg sleeves and then rested in supine position for at least 15 min to achieve a physiological steady state. Subsequently, the pump was started and the progressive inflation of the sleeves was typically completed in 5 min. At the end of inflation, the target pressure profile was kept constant for 5 min until the pressure was released rapidly on manual command. Participants remained in supine position for another 10 min with no external pressure applied to their legs. A schematic overview of the applied pressure timing is shown in figure 1.

Data acquisition

CMR imaging

Cardiac magnetic imaging was performed on a 1.5 T Ingenia MR scanner (Philips Medical Systems, Best, the Netherlands) using a phased-array cardiac coil.

Short-axis, two-chamber, and four-chamber view cine-loops were acquired before the leg compression using standard retrospectively vectorcardiographically-triggered steady-state free precession sequences at end-expiratory breath hold in order to assess left ventricular (LV) end-diastolic volume, end-systolic volume, and ejection fraction. Stroke volume (SV) was repeatedly measured using phase-contrast MRI; to this end, a retrospective, gated fast-field echo sequence with a 20° flip angle and a TR of 5 ms across the ascending aorta was used.

DCE-MRI images in four-chamber view were acquired using a non-steady state spoiled fast-gradient echo sequence; T1-weighting was achieved by a non-slice-selective saturation pre-pulse applied 85 ms before the acquisition. Acquisition was triggered in mid-diastole to minimize the effect of cardiac motion; the dynamic measurement was performed at end-expiratory breath-hold. Typically, a flip angle of 25° was used with a TR/TE of 6/2.9 ms, resulting in a typical voxel size of $1.6 \times 1.6 \times 10\,\text{mm}^3$; parallel imaging and undersampling were used to decrease image acquisition time to approximately 150 ms.

Repeated injections of 0.2 mmol of Dotarem (Guerbet) were administered intravenously using an automated MR injector (Medrad, Indianapolis). The CA bolus was diluted into 5 ml saline solution and injected at the rate of $5\,\text{ml}\,\text{s}^{-1}$, followed by a saline flush of 15 ml. Under these conditions, a linear relationship between CA concentration and MR signal was expected (Mischi *et al* 2009). Following the injection, a dynamic series of at least 45 images was

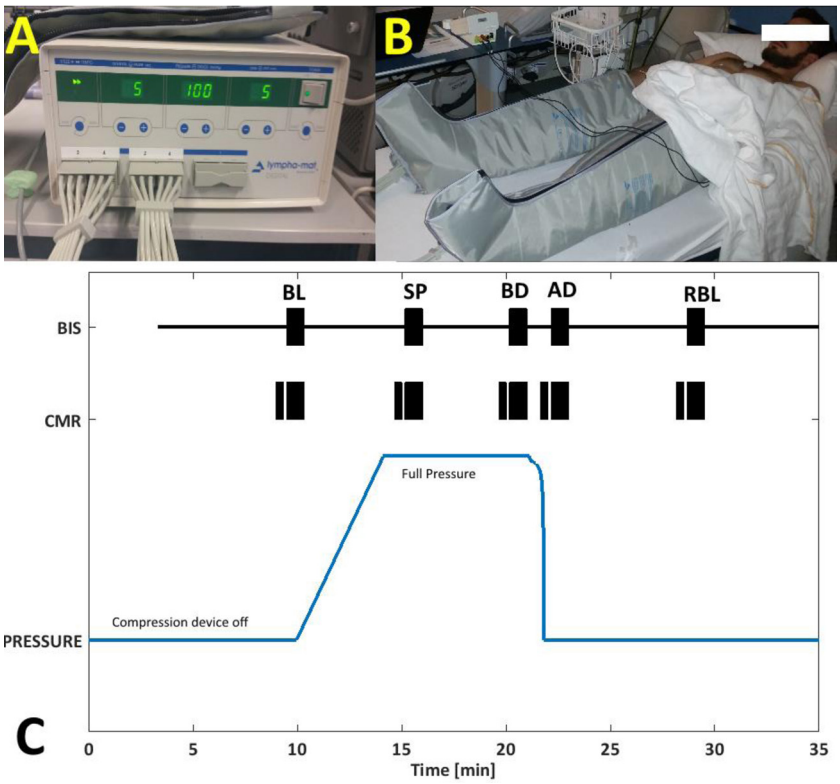

Figure 1. Leg compression device and measurement protocol. Picture of Lympha-mat Digital pump (A) with corresponding leg sleeves inflated around a subject (B). Schematic illustration of the external leg compression protocol repeated during the bio-impedance spectroscopy (BIS) and cardiac magnetic resonance (CMR) measurement sessions (C). The blue line indicates the timing of the gradual pressure build-up during the inflation of the leg sleeves and of the rapid pressure release. The black rectangles represent periods of end-expiratory breath hold at baseline (BL), steady pressure (SP), before deflation (BD), after deflation (AD) and return to baseline (RBL) included in both measurement sessions. CMR measurements were acquired intermittently during breath hold and BIS data was acquired continuously as indicated by the black line. Only data acquired during end-expiratory breath was used in the analysis.

acquired. In order to minimize the reciprocal influence between the repeated phase-contrast MRI and DCE-MRI measurements, a free breathing period of 20 s was allowed between the two measurements.

Bio-impedance spectroscopy

Monitoring of TI was performed using the commercial BIS device SFB7 (ImpediMed Ltd, Brisbane, Australia). The device measures bio-impedance at 256 frequencies in the range 3–1000 kHz using a tetra polar electrode configuration: two electrodes are used for the application of an excitation current, and two for voltage measurements. The electrodes were placed on both sides of the chest, along the axillary lines at the level of the 5th intercostal spaces (figure 2). The distance between neighboring electrodes was approximately 5 cm. The location of the electrodes was selected to achieve maximal sensitivity to pulmonary fluid (Wang *et al*

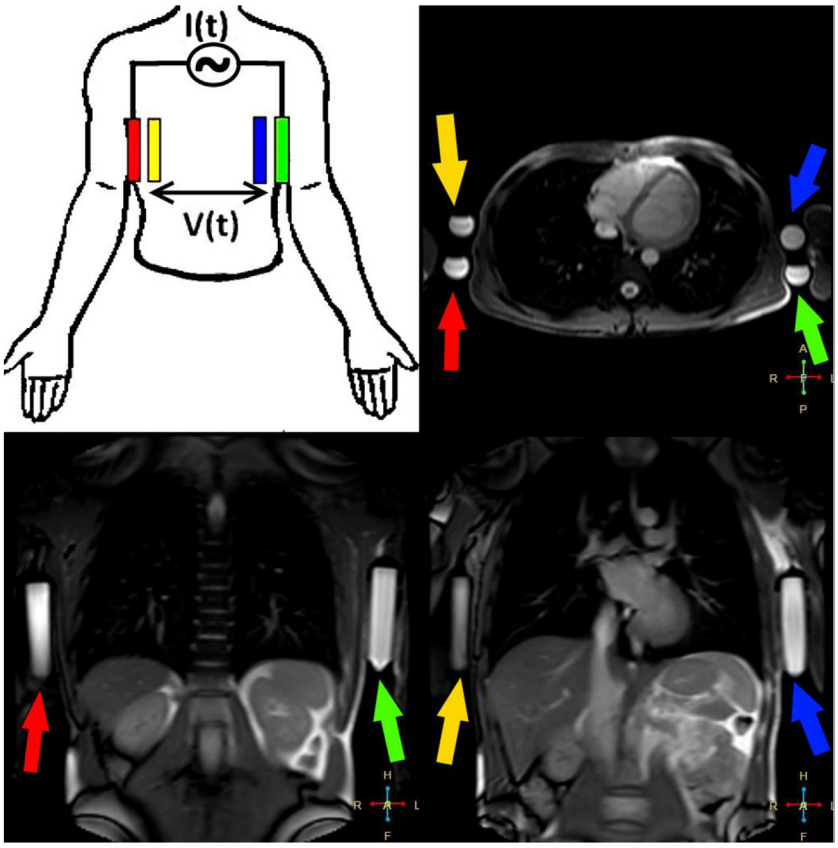

Figure 2. Electrode placement for tetra-polar bio-impedance spectroscopy (BIS) measurements. (a) Schematic illustrating the placement of the electrode pairs used for current injection (red and green) and voltage measurements (yellow and blue) during the BIS measurement session. (b)–(d) MRI views showing the position of the electrodes. Vials filled with saline solution saturated MRI contrast agent (concentration higher than 4 mmol) where attached to the thorax to show the position of the electrodes in the MR images. Colored arrows mark the correspondence between the schematic and the images.

2001, Beckmann *et al* 2007). Monitoring consisted of continuous BIS measurements at a rate of 40 bio-impedance spectra min^{-1}.

The TI session was designed to resemble the CMR session to facilitate an *a posteriori* comparison of the two measurement techniques. Monitoring of TI was performed in supine position and subjects were asked to perform end-expiratory breath hold at the same predefined time instances as in the CMR session (figure 1). Although TI measurements can be performed during normal breathing, the periods of end-expiratory breath hold enabled the acquisition of TI data without respiratory variations.

Timing of the measurements

Figure 1 illustrates the timing of the measurements performed before, during, and after the external leg compression. While BIS measurements were continuously acquired during the whole compression procedure, CMR measurements were performed intermittently at five time

intervals: before the beginning of the compression (baseline—BL), when the full pressure was reached (steady pressure—SP), after 300 s of maintained full pressure (before deflation—BD), 20 s after the abrupt pressure release (after deflation—AD), and 300 s after the deflation (return to baseline—RBL).

Data analysis

Cardiovascular magnetic resonance

Ventricular volumes were determined by semi-automatic tracking of the endocardial borders in the short-axis images and correcting for longitudinal shortening using CAAS MRV 3.4 (Pie Medical Imaging BV, Maastricht). CAAS Flow 1.2 (Pie Medical Imaging) was used to semi-automatically draw regions of interest in the aorta and derive the SVs.

Regions of interest were manually traced onto the DCE-MRI images series in the right ventricle (RV) and LV blood pools; IDCs were derived averaging in space the MR signal intensity within the region for each frame.

The local density random walk (LDRW) kinetic model was used to characterize the trans-pulmonary dilution process (Bogaard *et al* 1986). The model expression is:

$$S(t) = A\sqrt{\frac{\lambda\mu}{2\pi t}}\, \mathrm{e}^{-\frac{\lambda}{2}\left(\frac{t}{\mu}+\frac{\mu}{t}\right)}$$

where S(t) is the MR signal intensity, μ is the mean transit time, λ is a skewness parameter that relates to the Peclet number, A is a normalizing factor, and t is the time referred to as the theoretical injection time. It can be shown that this model constitutes a solution of the drift-diffusion equation (Bogaard *et al* 1986). The LDRW model was fitted to the obtained IDCs using an iterative Levenberg–Marquardt algorithm (Mischi *et al* 2004).

Intra-thoracic transit time (ITT) was defined as the difference between the mean transit time of the LV IDC and of the RV IDC. Intra-thoracic blood volume (ITBV) was obtained by multiplication of ITT by cardiac output (CO) assessed by phase-contrast MRI; ITBV and ITT were the CMR-derived measures of thoracic fluids considered in this study. Analysis of the DCE-MRI images and derived IDCs was performed using custom-made software in Matlab® 2015b (Natick, MA, USA).

Bio-impedance spectroscopy

The Cole–Cole model was used to describe the frequency dependent behavior of tissue bio-impedance as illustrated in figure 3. The model expression is (Cole and Cole 1941):

$$Z(f) = (R_{\mathrm{E}} \| R_{\mathrm{I}}) + \frac{R_{\mathrm{E}} - (R_{\mathrm{E}} \| R_{\mathrm{I}})}{1 + (j2\pi f (R_{\mathrm{E}} + R_{\mathrm{I}}) C_{\mathrm{M}})^{\alpha}}$$

The model parameters reflect extracellular fluids (R_{E}), intracellular fluids (R_{I}), the capacitive behavior of the cell membranes (C_{M}), and tissue heterogeneity (α). All four parameters were determined from the acquired bio-impedance data using the software BioImp 5.4 (ImpediMed Ltd, Brisbane, Australia). The software uses multiple linear regression to fit a semi-circle to the data in the complex impedance plane (Cornish *et al* 1993). In this study, the extrapolated parameter R_{E} (figure 3) was used as an indicator of intra-thoracic fluid content. We averaged the derived parameter values over the breath-hold intervals to minimize measurement errors and variability due to the cardiac cycle. The mean R_{E} value during breath hold was compared

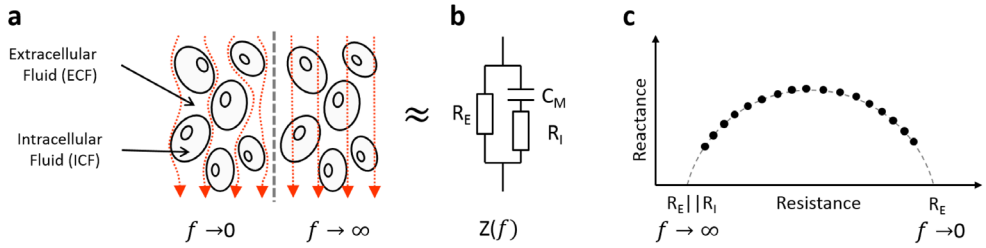

Figure 3. Principles of bio-impedance spectroscopy. (a) Flow of electrical current through biological tissue: low frequency currents flow around the cells through the extracellular fluid, and high-frequency currents flow through the extracellular fluid, cell membranes and intracellular fluid. (b) Equivalent electrical circuit of the tissue impedance ($Z(f)$) including the resistance of extracellular (R_E) and intracellular (R_I) fluids, and the capacitance of cell membranes (C_M) according to the Cole–Cole model; (c) Bio-impedance spectroscopy measurement points in the complex impedance plane and the extrapolated values of $Z(f)$ at low (R_E) and high ($R_E||R_I$) frequencies.

with CMR parameters. In order to reduce the inter-individual variability due to different body composition, we also normalized the obtained R_E value by the BMI of each subject. The analysis of the BIS data was performed in Matlab® 2015b (Natick, MA, USA).

Statistical methods

Continuous variables are presented as their mean and standard deviation. Changes in MRI and BIS parameters in the different time intervals during the leg-compression were compared using a paired t-test assuming unequal variance for the groups. A p-value smaller than 0.05 was considered statistically significant. Correlation between BIS and MRI derived parameters was expressed as Spearman correlation coefficient. ITBV and SV assessed by CMR were indexed to body surface area resulting in intra-thoracic blood volume index (ITBI) and stroke volume index (SVI). Body surface area was determined using the Du Bois formula (Du Bois and Du Bois 1989).

Results

A total of eight healthy volunteers were included in this study. Characteristics of the subjects are presented in table 1. Baseline values for the CMR and BIS considered parameters are shown in table 2.

Cardiovascular MR results

CMR was feasible in 38 out of the 40 (five intervals for each subject) planned time intervals. Two DCE-MRI measurements could not be performed due to problems in the contrast injection procedure. For one subject, the DCE-MRI during RBL measurement resulted in a low signal-to-noise ratio, reflected in a poor determination coefficient for the LV IDC LDRW fit ($R^2 < 0.7$); the measurement was therefore excluded from further analysis. Determination coefficients of the LDRW fits for the remaining cases ($n = 37$) were 0.98 ± 0.02 for the LV IDC and 0.98 ± 0.03 for the RV IDC, respectively. An example of CMR based ITBV measurement is shown in figure 4.

Table 1. Demographics and general characteristics of the included population.

Variable	Value
Gender: male/female	8/0
Age, years	39 ± 13
BMI, kg m^{-2}	23.9 ± 2.3
BSA, m^2	1.95 ± 0.12
Creatinine clearance, ml min^{-1}	80.0 ± 8.4
LVEDVI, ml m^{-2}	68.5 ± 12.8
LVESVI, ml m^{-2}	27.7 ± 9.0
LVEF, %	60.4 ± 7.4

BMI, body mass index; BSA, body area surface; LVEDVI, left ventricular end-diastolic volume index; LVESVI left ventricular end-systolic volume index; LVEF, left ventricular ejection fraction.

Table 2. Magnetic resonance imaging and bio-impedance spectroscopy derived parameters at baseline.

Variable	Value
CMR-SVI, ml m^{-2}	45.3 ± 5.1
CMR-HR, beats min^{-1}	61.9 ± 6.0
CMR-CI, l (min $\cdot$ m^2)$^{-1}$	2.79 ± 0.25
CMR-ITBI, ml m^{-2}	352.2 ± 37.0
BIS-R_E, Ω	50.6 ± 5.7

CMR, cardiac magnetic resonance, SVI, stroke volume index; HR, heart rate; CI, cardiac index; ITBI, intra-thoracic blood volume index; BIS-R_E, extracellular resistance derived from bio-impendance spectroscopy.

The observed changes in aortic flow assessed by phase-contrast MRI, and in IDCs derived from DCE-MRI recordings for one subject are shown in figure 5.

We observed changes of 45.2 ± 47.2 ml m^{-2} in ITBI by CMR when comparing BL and SP (significantly different, $p < 0.05$), and of 30.6 ± 34.7 ml m^{-2} when comparing BL and BD ($p < 0.05$). After release of the pneumatic pressure the ITBI changes were respectively -29.4 ± 24.4 ml m^{-2} ($p < 0.05$) and -26.6 ± 31.2 ml m^{-2} ($p < 0.05$) when comparing BD with AD and RBL, respectively.

When normalizing the ITBI changes to the baseline value for each individual, the change in ITBI after inflation was $13.1 \pm 15.1\%$ (BL to SP, statistically significant increase, $p < 0.05$), while the decrease after deflation (BD to RBL) was $-7.2 \pm 9.3\%$ (statistically significant decrease, $p < 0.05$).

When considering the SVI, the increase after inflation (BL to SP) was 3.2 ± 5.0 ml m^{-2} ($p > 0.20$), while the change in ITT was 0.11 ± 0.66 s ($p > 0.68$). After deflation (BD to RBL), the changes were -1.5 ± 4.9 ml m^{-2} for SVI ($p > 0.34$), and for -0.3 ± 0.8 s ITT ($p > 0.29$), respectively. For the heart rate, the change after inflation (BL to SP) was 2.1 ± 5.4 s^{-1} ($p > 0.33$), while after the deflation (BD to RBL) was 0.7 ± 3.8 s^{-1} ($p > 0.61$).

BIS results

Examples of multi-frequency bio-impedance data acquired during different time intervals (BL and SP) of the leg compression protocol and the corresponding Cole–Cole model is shown in

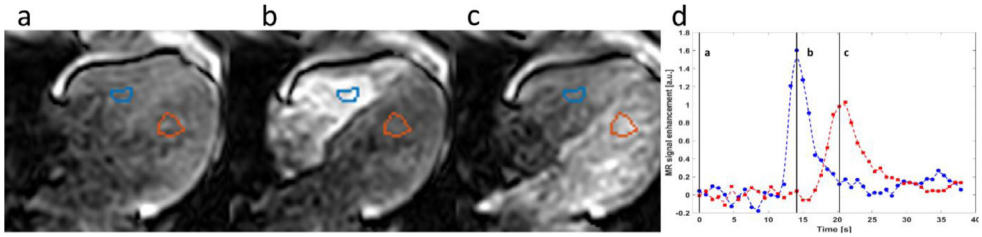

Figure 4. Example of four chamber view DCE-MRI images and corresponding indicator dilution curves (IDCs). Left to right: four chamber view before contrast agent passage (a), during contrast agent passage in right (b) and left (c) ventricle (RV and LV, respectively), with overlaid region of interest (blue—RV ROI, red LV ROI). Corresponding IDCs (d) derived averaging the signal intensity within the ROIs per frame (blue curve RV IDC, red curve LV IDC). Vertical lines represent the timing of the depicted images (a)–(c).

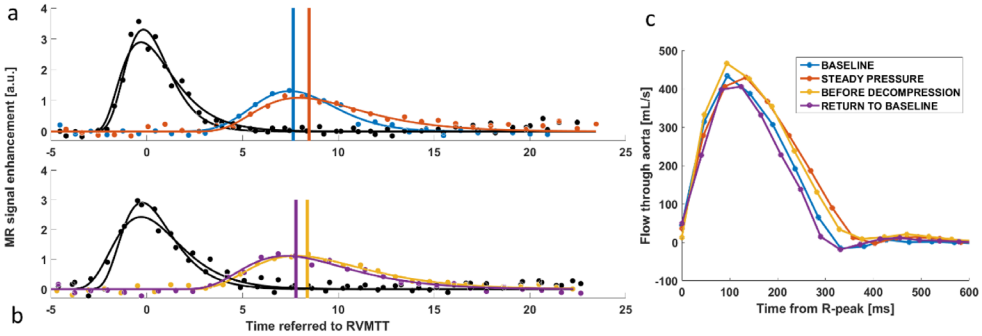

Figure 5. Typical changes in acquired magnetic resonance imaging (MRI) data during leg compression. Changes in left ventricular (LV) indicator dilution curves (IDCs) before (blue) and after the compression (orange) (a), changes in LV IDCs before (yellow) and after (purple) deflation (b); for easier visual comparison, time-scale refers to the time passed since right ventricular mean transit time (RVMTT) for all the measurements. Change in aortic blood flow assessed by phase-contrast MRI (c) at the different time intervals during the leg compression procedure (same color as IDCs). Vertical lines in (a) and (b) indicate the intra-thoracic transit time in the different phases (same color as IDCs).

figure 6(a). Figure 6(b) shows an example of R_E variation during the entire BIS measurement session of a subject.

In the overall study group we observed changes in R_E of $-0.84 \pm 0.39\ \Omega$ (BL to SP, $p < 0.001$), $-0.15 \pm 0.20\ \Omega$ (BL to BD, $p < 0.05$), $0.52 \pm 0.35\ \Omega$ (BD to AD, $p < 0.01$), and $0.59 \pm 0.45\ \Omega$ (BD to RBL, $p < 0.01$). When normalizing the R_E measures to the baseline value for each individual, the decrease after inflation was $-1.7 \pm 0.9\%$ ($p < 0.05$), while the increase after deflation was $1.2 \pm 0.9\%$ ($p < 0.05$).

Comparison of BIS and CMR results

Changes in ITBI, derived from CMR measurements, and in R_E, obtained by BIS model fit, normalized as % of baseline values are shown in boxplots in figure 7.

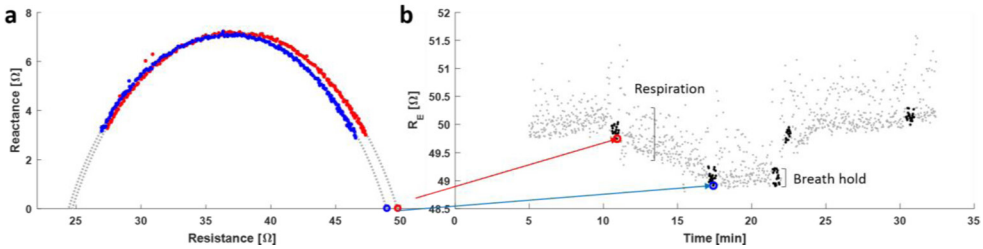

Figure 6. Typical variations in bio-impedance spectroscopy (BIS) data. (a) Bio-impedance spectra before (red) and during (blue) external leg compression. (b) Evolution of R_E in one subject throughout a BIS measurement session including periods of free breathing and end-expiratory breath hold. Black dots are values obtained during end-expiratory breath hold before, during and after the leg compression procedure. The red and blue circles mark the correspondence with the bio-impedance spectra in (a).

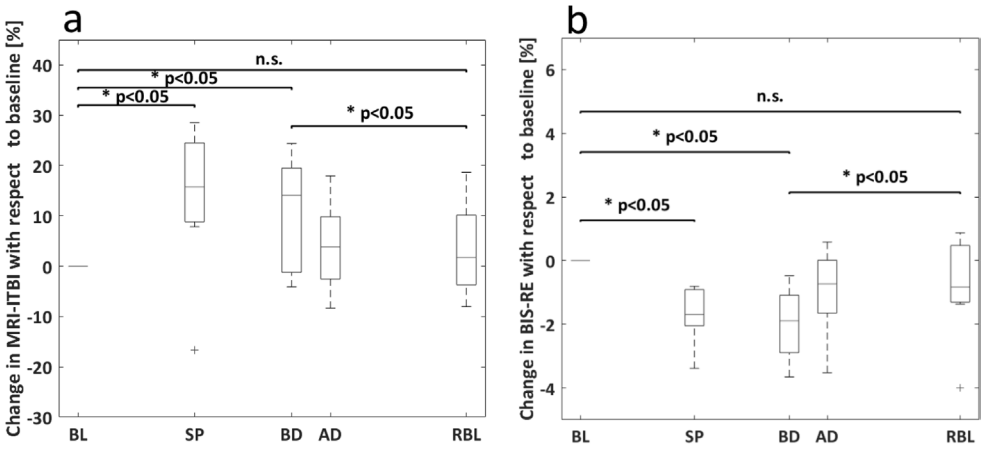

Figure 7. Normalized changes during leg compression shown as boxplots. Changes in intra-thoracic blood volume index (ITBI) measured by MRI for all subjects ($n = 8$) during the different phases of the leg compression protocol (a) (BL = baseline, SP = steady pressure, BD = before deflation, AD = after deflation, RBL = return to baseline). Changes in extracellular resistance (R_E) in the same time instants in the compression procedure obtained by Cole–Cole model fitting of the bio-impedance spectroscopy (BIS) data (b). (* = paired Student's t-test, n.s. = not significant).

ITT and R_E normalized by BMI (R_En) at baseline correlated well ($r = -0.92$, $p < 0.005$), as shown in figure 8. ITBV and R_En were also significantly correlated at baseline ($r = -0.93$, $p < 0.005$ for ITBV, $r = -0.73$, $p < 0.05$ when considering ITBI). Correlation between ITT (ITBV) and BMI was not significant, $p > 0.70$ ($p > 0.42$).

Changes in ITT and R_E during deflation transition (BD to RBL) were correlated ($r = 0.75$, $p < 0.05$) as shown in figure 8. Correlation between changes in ITT and changes in R_E during other transitions were not significant.

Discussion

Purpose of this study was to evaluate and compare the changes in physiological parameters measured by BIS and CMR in response to acute fluid displacement induced by application of external pneumatic pressure on the lower extremities.

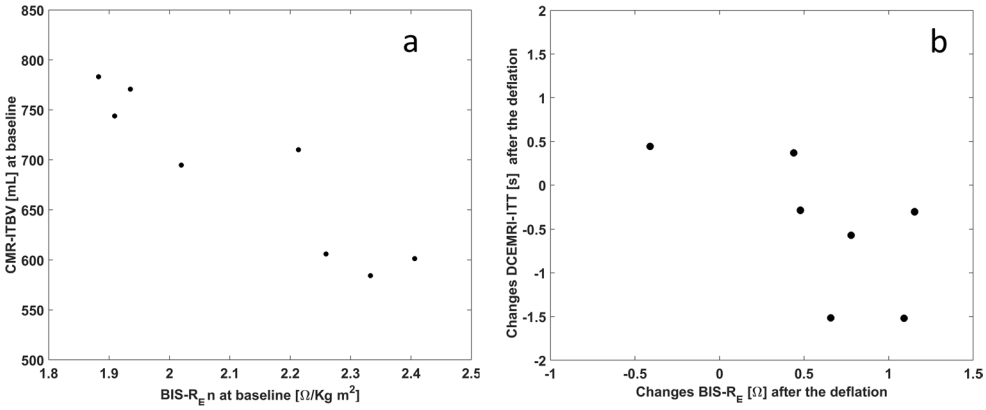

Figure 8. Comparison between bio-impedance spectroscopy (BIS) and cardiac magnetic resonance imaging (CMR) measures. (a) Comparison between intra-thoracic blood volume (ITBV) measured by CMR and extracellular resistance (R_E) normalized to body mass index (BMI) baseline values for all subjects ($n = 8$);(b) comparison between absolute changes in intra-thoracic transit time (ITT) and R_E from before deflation to return to baseline.

Repeated DCE-MRI measurement during the leg compression was feasible in volunteers. However, the response to sleeves deflation was accompanied by an increase in heart rate caused by a baroreceptor reflex to buffer the sharp decrease in blood pressure (Randall *et al* 1984); this caused problematic electrocardiographic trigger for the CMR measurement, resulting in inconsistent measurement timing. We therefore excluded from the analysis the AD measurement. The baseline ITBI measured by DCE-MRI is in line with previous findings reported by Milnor *et al* (1960), where an indexed volume of 365 ml m^{-2} was measured by a dye-dilution method and simultaneous bilateral cardiac catheterization in healthy volunteers.

BIS and CMR measurements were performed within 2 hours in each subject to exclude slow fluid status changes, e.g. related to dietary fluid intake. The adopted dose of MR CA was small compared to clinically approved doses for perfusion studies (Thomsen 2007), to minimize adverse effects and potential accumulation of the CA. The possible mutual influence of phase contrast-MRI and DCE-MRI measurements has been shown to be minimal in the literature (Makowski *et al* 2015). We used a pneumatic leg compression for lymphedema therapy as a non-invasive means to achieve a reversible displacement of blood volume from the legs towards the thorax. Unlike lymphedema therapy consisting of repeated inflation cycles with the pressure released seconds after the end of inflation, we maintained the pressure for a longer duration (5 min) in order to perform measurements. To maximize the displaced blood volume we applied high pressures (60–100 mmHg) to the individual chambers of the sleeves, with a pressure gradient along each leg to minimize the perceived discomfort associated with the prolonged compression at high pressures.

When applying external compression to the legs, we observed a significant decrease in thoracic R_E which, according to the Cole–Cole model, reflects an increase in extracellular fluid volume that lowers the opposition of thoracic tissues to the flow of electric current. The increase in extracellular fluids in the thorax is most likely associated with the displacement of blood volume including blood plasma, i.e. extracellular fluid from the legs towards the upper body. We have also observed an increase in ITBI measured by CMR. Both effects appeared reversible as both BIS and CMR parameters returned to baseline values after the release of the

external pressure. No significant changes were observed between the repeated measurements performed during the pressure hold time (SP and BD); this may be due to the relatively small sample size, not sufficient to elucidate the physiological adaption to the applied pressure, and the corresponding inter-subject variability in the adaption.

The presented results suggest that the proposed measurement techniques are sensitive to acute blood displacement in healthy volunteers. However, the inter-subject variability of these effects was relatively large; possible factors to explain this variability may include the different mental distress experienced by the subjects during the procedures (Carter *et al* 2005), and the nociceptive stimulation (Randall *et al* 1984) caused by the compression, which are known to influence peripheral vasculature status.

In the literature, there is general agreement that pneumatic leg compression results in increase of SV and CO (Randall *et al* 1984). It is also known from the literature that rapid application of 100 mmHg pressure over the surface of the body by means of anti-shock trousers causes acute, reversible redistribution of blood from peripheral vasculature to the central circulation in normal man (Bondurant *et al* 1957, Bivins *et al* 1982). In particular, Bondurant *et al* (1957) evidenced this effect by observing an increase in radiographic density of the lungs and in thoracic radioactivity after injection of labeled albumin. Tenney and Honig (1955) calculated a displacement of 250 ml of blood in normal subjects at 40 mmHg inflation by measuring displacement of the center of gravity in subjects. Similar figures for the blood displaced volume (from 210 to 450 ml) were estimated from Hanke (1985). Our results are inline, although we observed a relatively smaller average increase in the order of 90 ml in the pulmonary circulation. It is reasonable to expect that the blood displaced from the legs did not only distribute to the pulmonary circulation but also to other vascular networks in the upper body. Other authors suggested that a larger volume (750–1000 ml) of blood was displaced from the lower body, into the upper body (Randall *et al* 1984). However, their findings were in context of hemorrhagic patients, a severely impaired hemodynamic scenario which may not generalize in healthy volunteers.

The proposed experimental design could be further exploited for improving the understanding of pulmonary hemodynamics; in particular, further research would be needed to investigate the extent and the temporal dynamics of the physiological adaptation to the applied external pressure. It has been noticed that, in controlled experiments, during pure blood displacement the impedance spectrum does not fit the simple depressed Cole–Cole circle at high frequencies, suggesting further frequency dependent conduction properties of the erythrocytes (Scharfetter *et al* 1997). Clinical utility of BIS measurement could be increased if frequency-dependent markers for blood instead of general fluid content could be identified. The combined use of purely intravascular and extravascular imaging CA may provide a validation strategy for this phenomenon.

We suggest that a combination of BIS and CMR measurements should be prospectively tested for its ability to predict re-hospitalization after admission for HF. Direct blood volume measurement offers complementary information that could improve the clinical usefulness of serial TI measurements obtained during a follow-up period. Absolute volume measurements might be used to ‘calibrate’ the TI measurement, normalizing its baseline value, and potentially improving clinical decision making based on subsequent BIS measurements (Katz 2007). For instance, TI-based early warning systems may be programmed to achieve high sensitivity to fluid congestion in order to identify patient episodes which may lead to hospitalization. An inherent number of unnecessary interventions due to false alarms may be reduced through personalization of TI-based early warning systems with patient-specific thresholds. Personalization may be achieved by direct volume assessments in each patient during the initialization phase of the TI warning system or based on models of the relationship between

absolute fluid volumes, TI, and anthropomorphic characteristics e.g. chest geometry and composition. Both BIS and CMR have potential for discriminating the intra- and extra-vascular thoracic fluid status, not evaluated in this work. Further research is therefore needed to fully characterize the possibly nonlinear relationship between BIS and CMR parameters.

Limitations

Limitation of the study was the prolonged end-expiratory breath hold required for the CMR measurement, which is subjective and it may be challenging to obtain consistently in HF patients. Moreover, CMR is generally costly and gadolinium based CA may introduce risks when renal function is impaired. However, contrast-enhanced ultrasound is a valid alternative for blood volume assessment (Herold *et al* 2016a), with purely intravascular ultrasound CAs associated with lower side effects (Bommer *et al* 1984). Additionally, ultrasound allows indicator dilution measurement in free breathing, with results in good agreement with CMR (Herold *et al* 2016b).

Conclusions

An acute and reversible displacement of blood from the lower extremities to the thoracic circulation was induced in normal subjects by external leg compression. During compression, significant changes were observed in the physiological parameters derived from BIS and CMR measurements. Consistent changes with opposite trends were observed when the pressure was released. A good correlation was observed between R_E derived from BIS and ITBV assessed by DCE-MRI. Further research is needed to fully characterize the relationship between changes in CMR and BIS measures of fluid content and to evaluate the feasibility of CMR-based BIS patient-specific calibration.

Acknowledgments

This research was supported by the Dutch Technology Foundation STW with Open Technology Program (OTP) grant 11865.

The authors acknowledge G Wahyulaksana, for his assistance in implementing the leg compression protocol, and M Kohler, for operating the MRI scanner. The authors thank M Castello from Istituto Italiano di Tecnologia for the fruitful discussions.

References

Abraham W T *et al* 2011 Intrathoracic impedance versus daily weight monitoring for predicting worsening heart failure events: results of the fluid accumulation status trial (FAST) *Congestive Heart Failure* **17** 51–5

Adamson P B *et al* 2003 Ongoing right ventricular hemodynamics in heart failure: clinical value of measurements derived from an implantable monitoring system *J. Am. Coll. Cardiol.* **41** 565–71

Aime S and Caravan P 2009 Biodistribution of gadolinium-based contrast agents, including gadolinium deposition *J. Magn. Reson. Imaging* **30** 1259–67

Beckmann L, Van Riesen D and Leonhardt S 2007 Optimal electrode placement and frequency range selection for the detection of lung water using bio-impedance spectroscopy *Proc. Annual Int. Conf. of the IEEE Engineering in Medicine and Biology Society* pp 2685–8

Bera T K 2014 Bioelectrical impedance methods for noninvasive health monitoring: a review *J. Med. Eng.* **2014** 381251

Bivins H G, Knopp R, Tiernan C, dos Santos P A and Kallsen G 1982 Blood volume displacement with inflation of anti-shock trousers *Ann. Emerg. Med.* **11** 409–12

Blair J E A *et al* 2009 Weight changes after hospitalization for worsening heart failure and subsequent re-hospitalization and mortality in the EVEREST trial *Eur. Heart J.* **30** 1666–73

Bogaard J M, Jansen J R C, von Reth E A, Versprille A and Wise M E 1986 Random walk type models for indicator-dilution studies: comparison of a local density random walk and a first passage times distribution *Cardiovasc. Res.* **20** 789–96

Bolton M P *et al* 1998 Sources of error in bio-impedance spectroscopy *Physiol. Meas.* **19** 235–45

Bommer W J, Shah P M, Allen H, Meltzer R and Kisslo J 1984 The safety of contrast echocardiography: report of the Committee on Contrast Echocardiography for the American Society of Echocardiography *J. Am. Coll. Cardiol.* **3** 6–13

Bondurant B S, Hickam J B and Isley J K 1957 Pulmonary and circulatory effects of acute pulmonary vascular engorgement in normal subjects *J. Clin. Invest.* **36** 1–59

Carter J R, Kupiers N T and Ray C A 2005 Neurovascular responses to mental stress *J. Physiol.* **564** 321–7

Cassola V F, Lima V J, Kramer R and Khoury H J 2010 FASH and MASH: female and male adult human phantoms based on polygon mesh surfaces: I. Development of the anatomy *Phys. Med. Biol.* **55** 133–62

Chaudhry S I, Wang Y, Concato J, Gill T M and Krumholz H M 2007 Patterns of weight change preceding hospitalization for heart failure *Circulation* **116** 1549–54

Cole K S and Cole R H 1941 Dispersion and absorption in dielectrics I. Alternating current characteristics *J. Chem. Phys.* **9** 341

Conraads V M, Tavazzi L, Santini M, Oliva F, Gerritse B, Yu C M and Cowie M R 2011 Sensitivity and positive predictive value of implantable intrathoracic impedance monitoring as a predictor of heart failure hospitalizations: the SENSE-HF trial *Eur. Heart J.* **32** 2266–73

Cornish B H, Thomas B J and Ward L C 1993 Improved prediction of extracellular and total body water using impedance loci generated by multiple frequency bioelectrical impedance analysis *Phys. Med. Biol.* **38** 337

Cotter G, Metra M, Milo-Cotter O, Dittrich H C and Gheorghiade M 2008 Fluid overload in acute heart failure—re-distribution and other mechanisms beyond fluid accumulation *Eur. J. Heart Failure* **10** 165–9

Dovancescu S, Torabi A, Mabote T, Caffarel J, Kelkboom E, Aarts R, Korsten E and Cleland J 2013 Sensitivity of a wearable bio-impedance monitor to changes in the thoracic fluid content of heart failure patients *Comput. Cardiol.* **40** 927–30

Du Bois D and Du Bois E F 1989 A formula to estimate the approximate surface area if height and weight be known. 1916 *Nutrition* **5** 303

Gattis W A, O'Connor C M, Gallup D S, Hasselblad V and Gheorghiade M 2004 Predischarge initiation of carvedilol in patients hospitalized for decompensated heart failure: results of the initiation management predischarge: process for assessment of carvedilol therapy in heart failure (IMPACT-HF) trial *J. Am. Coll. Cardiol.* **43** 1534–41

Gheorghiade M *et al* 2010 Assessing and grading congestion in acute heart failure: a scientific statement from the acute heart failure committee of the heart failure association of the European Society of Cardiology and endorsed by the European Society of Intensive Care Medicine *Eur. J. Heart Failure* **12** 423–33

Gheorghiade M *et al* 2012 A comprehensive, longitudinal description of the in-hospital and post-discharge clinical, laboratory, and neurohormonal course of patients with heart failure who die or are re-hospitalized within 90 d: analysis from the EVEREST trial *Heart Failure Rev.* **17** 485–509

Gyllensten I C, Bonomi A G, Goode K M, Reiter H, Habetha J, Amft O and Cleland J G 2016a Early indication of decompensated heart failure in patients on home-telemonitoring: a comparison of prediction algorithms based on daily weight and noninvasive transthoracic bio-impedance *JMIR Med. Inform.* **4** e3

Gyllensten I C, Paloma Gastelurrutia P, Bonomi A G, Riistama J, Bayes-Genis A and Aarts R M 2016b A method to adapt thoracic impedance based on chest geometry and composition to assess congestion in heart failure patients *Med. Eng. Phys.* **38** 538–46

Hanke B K, Bivins H G, Knopp R and dos Santos P A 1985 Anti- shock trousers: a comparison of inflation techniques and inflation pressures *Ann. Emerg. Med.* **14** 636–40

Harabis V, Kolar R, Mezl M and Jirik R 2013 Comparison and evaluation of indicator dilution models for bolus of ultrasound contrast agents *Phys. Meas.* **34** 151–62

Heist E K *et al* 2014 Analysis of different device-based intrathoracic impedance vectors for detection of heart failure events (from the detect fluid early from intrathoracic impedance monitoring study) *Am. J. Cardiol.* **114** 1249–56

Herold I H F, Saporito S, Bouwman R A, Houthuizen P, van Assen H C, Mischi M and Korsten H H 2016a Reliability, repeatability, and reproducibility of pulmonary transit time assessment by contrast enhanced echocardiography *Cardiovasc. Ultrasound* **14** 1

Herold I H F *et al* 2016b Pulmonary transit time measurement by contrast-enhanced ultrasound in left ventricular dyssynchrony *Echo Res. Pract.* **3** 35–43

Henderson A C, Prisk G K, Levin D L, Hopkins S R and Buxton R B 2009 Characterizing pulmonary blood flow distribution measured using arterial spin labeling *NMR Biomed.* **22** 1025–35

Jaffrin M Y, Massarani M, Le Gouerrier A and Boudailliez B 1997 Extra- and intracellular volume monitoring by impedance during haemodialysis using Cole–Cole extrapolation *Med. Biol. Eng. Comput.* **35** 266–70

Jaffrin M Y and Morel H 2008 Body fluid volumes measurements by impedance: a review of bio-impedance spectroscopy (BIS) and bio-impedance analysis (BIA) methods *Med. Eng. Phys.* **30** 1257–69

Kanai H, Haeno M and Sakamoto K 1987 Electrical measurement of fluid distribution in legs and arms *Med. Prog. Technol.* **12** 159–70

Karamitsos T D, Francis J M, Myerson S, Selvanayagam J B and Neubauer S 2009 The role of cardiovascular magnetic resonance imaging in heart failure *J. Am. Coll. Cardiol.* **54** 1407–24

Katz S D 2007 Blood volume assessment in the diagnosis and treatment of chronic heart failure *Am. J. Med. Sci.* **334** 47–52

Kushner R 1992 Bioelectrical impedance analysis: a review of principles and applications *J. Am. Coll. Nutrition* **11** 199–209

Lakoma A, Tuite D, Sheehan J, Weale P and Carr J C 2010 Measurement of pulmonary circulation parameters using time-resolved MR angiography in patients after Ross procedure *Am. J. Roentgenol.* **194** 912–9

Makowski M R, Wiethoff A J, Ebersberger H U, Botnar R M, Razavi R, Schaeffter T and Greil G F 2015 2D phase contrast blood flow velocity measurements of the thoracic vasculature: comparison of the effect of gadofosveset trisodium and gadopentetate dimeglumine *Int. J. Cardiovasc. Imaging* **31** 409–16

Medrano G, Beckmann L, Zimmermann N, Grundmann T, Gries T and Leonhardt S 2007 Bio-impedance spectroscopy with textile electrodes for a continuous monitoring application *Proc. 4th Int. Workshop on Wearable and Implantable Body Sensor Networks* vol 13, pp 23–8

Milnor W R, Jose A D and Mcgaff C J 1960 Pulmonary vascular volume, resistance, and compliance in man *Circulation* **22** 130–7

Mischi M, Kalker T A and Korsten H H M 2004 Contrast echocardiography for pulmonary blood volume quantification *IEEE Trans. Ultrason. Ferroelectr. Freq. Control* **51** 1137–47

Mischi M, van den Bosch H C M, den Boer J A, Verwoerd J, Grouls R J E, Peels C H and Korsten H H M 2009 Intra-thoracic blood volume measurement by contrast magnetic resonance imaging *Magn. Reson. Med.* **61** 344–53

Moissl U M *et al* 2006 Body fluid volume determination via body composition spectroscopy in health and disease *Physiol. Meas.* **27** 921–33

Monnet X, Rienzo M, Osman D, Anguel N, Richard C, Pinsky M R and Teboul J 2006 Passive leg raising predicts fluid responsiveness in the critically ill *Crit. Care Med.* **34** 1402–7

O'Connor C M, Stough W G, Gallup D S, Hasselblad V and Gheorghiade M 2005 Demographics, clinical characteristics, and outcomes of patients hospitalized for decompensated heart failure: observations from the IMPACT-HF registry *J. Cardiac Failure* **11** 200–5

Picano E, Gargani L and Gheorghiade M 2010 Why, when, and how to assess pulmonary congestion in heart failure: pathophysiological, clinical, and methodological implications *Heart Failure Rev.* **15** 63–72

Pierson R N, Wang J, Colt E W and Neumann P 1982 Body composition measurements in normal man: the potassium, sodium, sulfate and tritium spaces in 58 adults *J. Chronic Dis.* **35** 419–28

Randall P, Banks J and Little R A 1984 Medical (military) anti-shock trousers-a short review *Arch. Emerg. Med.* **1** 39–51

Sakka S G, Rühl C C, Pfeiffer U J, Beale R, McLuckie A, Reinhart K and Meier-Hellmann A 2000 Assessment of cardiac preload and extravascular lung water by single transpulmonary thermodilution *Intensive Care Med.* **26** 180–7

Sasaki S, Ishida Y, Kinjo T, Itoh T, Horiuchi D, Sasaki K, Owada S, Kimura M and Okumura K 2013 Telediagnosis of heart failure with continuous intrathoracic impedance monitoring by Medtronic Carelink Network: importance of the elevation pattern of OptiVol Fluid Index *J. Arrhythmia* **29** 347–52

Scharfetter H, Monif M, László Z, Lambauer T, Hutten H and Hinghofer-Szalkay H 1997 Effect of postural changes on the reliability of volume estimations from bio-impedance spectroscopy data *Kidney Int.* **51** 1078–87

Schloerb P R, Friis-Hansen B J, Edelman I S, Solomon A K and Moore F D 1950 The measurement of total body water in the human subject by deuterium oxide dilution *J. Clin. Invest.* **29** 1296–310

Slutsky R A, Bhargava V and Higgins C B 1983 Pulmonary circulation time: comparison of mean, median, peak, and onset (appearance) values using indocyanine green and first-transit radionuclide techniques *Am. Heart J.* **106** 41–5

Stewart G N 1921 The pulmonary circulation time, the quantity of blood in the lungs and the output of the heart *Am. J. Physiol.* **58** 20–44

Tenney S M and Honig C R 1955 The effect of the anti-G suit on the ballistocardiogram: reversal of normal respiratory variation and change in thoracic blood volume *J. Aviat. Med.* **26** 194–9

Thomsen H S 2007 ESUR guideline: gadolinium-based contrast media and nephrogenic systemic fibrosis *Eur. Radiol.* **17** 2692–6

van Veldhuisen D J *et al* 2011 Intrathoracic impedance monitoring, audible patient alerts, and outcome in patients with heart failure *Circulation* **124** 1719–26

Wang Y, Haynor D R and Kim Y 2001 A finite-element study of the effects of electrode position on the measured impedance change in impedance cardiography *IEEE Trans. Biomed. Eng.* **48** 1390–401

Weyer S, Zink M D, Wartzek T, Leicht L, Mischke K, Vollmer T and Leonhardt S 2014 Bioelectrical impedance spectroscopy as a fluid management system in heart failure *Physiol. Meas.* **35** 917–30

Wong D T, Lee K J, Yoo S J, Tomlinson G and Grosse-Wortmann L 2014 Changes in systemic and pulmonary blood flow distribution in normal adult volunteers in response to posture and exercise: a phase contrast magnetic resonance imaging study *J. Physiol. Sci.* **64** 105–12

Yancy C and Abraham W T 2003 Noninvasive hemodynamic monitoring in heart failure: utilization of impedance cardiography *Congestive Heart Failure* **9** 241–50

Yu C M, Wang L, Chau E, Chan R H W, Kong S L, Tang M O, Christensen J, Stadler R W and Lau C P 2005 Intrathoracic impedance monitoring in patients with heart failure *Circulation* **112** 841–8

Zlochiver S, Arad M, Radai M M, Barak-Shinar D, Krief H, Engelman T, Ben-Yehuda R, Adunsky A and Abboud S 2007 A portable bio-impedance system for monitoring lung resistivity *Med. Eng. Phys.* **29** 93–100